

Electromagnetic actuator design for the control of light structures

Johan Der Hagopian and Jarir Mahfoud*

Laboratoire de Mécanique des Contacts et des Structures- UMR CNRS 5259, Institut National des Sciences Appliquées de Lyon, France

(Received July 31, 2008, Accepted May 14, 2009)

Abstract. An ElectroMagnetic Actuator (EMA) is designed and assessed numerically and experimentally. The EMA has the advantage to be without contact with the structure so it could be applied to light and small mechanism. Nevertheless, the open-loop instability and the nonlinear dynamic behavior with respect to the excitation frequency could limit its application field. The EMA is designed and dimensioned as a function of the experimental structure to be controlled. An inverse model of the EMA is proposed in order to implement a linear action block for the used frequency range. The control strategy is a fuzzy controller with displacements and velocities as inputs. A fuzzy controller of Takagi-Sugeno type is used. The air gap is estimated by using a modal approximation of the displacements issued from all measurements. Several configurations of control are assessed by using numerical simulations. The block diagram used for numerical simulations is implemented under Dspace[®] environment. The implemented controller was tested experimentally in the context of impact perturbations. The results obtained show the effectiveness of the developed procedures and the robustness of the implemented control.

Keywords: electromagnetic actuator; fuzzy control; experiments; dynamic behavior.

1. Introduction

Active Magnetic Bearings have been (AMB) successfully applied in industrial turbomachinery (Schweitzer, *et al.* 2003). Their main advantages are contact-less working environment, no sealing constraints, frictionless suspension, and that they represent an active system. They are well suited to operate contact-less as actuator and sensor element in rotating machinery (Lei and Palazzolo, 2008, Kasarda, *et al.* 2007, Mani, *et al.* 2006 and Aenis, *et al.* 2002). Matsuzaki, *et al.* (2000) presented a concept of the control system in which vibrations of a partially magnetized thin beam are actively suppressed using electromagnetic forces induced by an electric current conducted through the beam, in this case the applications are limited to small and light structures. AMB devices in conjunction with conventional support bearings are utilized either as an active magnetic damper (Kasarda, *et al.* 2004, Liu and Liu 2008), or for controlling the instability of certain supports as journal bearings (El-Shafei and Dimitri 2007). This technology is also utilized for controlling non-rotating structures; in this case the AMB is considered as an ElectroMagnetic Actuator (EMA) and is utilized in many practical applications: electromagnetic valve actuators of combustion engines, artificial heart actuators, micropositioning systems, etc (Forrai, *et al.* 2007, Fung, *et al.* 2005 and Lee and Gweon 2000).

*Corresponding Author, E-mail: Jarir.mahfoud@insa-lyon.fr

Previous works investigated suitable procedures for controlling the dynamic behavior of rotating machinery while crossing critical speeds and instability zones. Couzon and Der Hagopian (2007) presented a neuro-fuzzy approach for the control of rotor suspended on active magnetic bearing; the control was achieved successfully for the rigid body modes. Simões, *et al.* (2007) demonstrated the possibility of controlling flexible body modes when crossing critical speeds by using piezoelectric actuators. The aim now is to investigate the possibilities of controlling structures by using EMA for their simple electromechanical structure and their contact-less properties. As a first step, an EMA is designed and characterized experimentally. And since a rotor at rest can initially be considered as a flexible beam, the possibility of controlling a flexible beam by using EMA is assessed numerically and experimentally.

EMA can only produce attractive electromagnetic force and has strongly nonlinear characteristics due to the fact that this electromagnetic force is current and armature position dependent. So EMAs are inherently instable and require closed-loop control for stable operation. For those reasons, the EMA is first designed and dimensioned as a function of the experimental structure to be controlled. Based on magnetic theory, an inverse model of the EMA, with current control configuration, is then proposed in order to implement a linear action block, for the used frequency range.

The control strategy is a fuzzy controller of Takagi-Sugeno type. It was found to be the well adapted for controlling flexible structures. Moreover, this type of controller has performance that allows taking into account slight nonlinearities and uncertainties due to the experimental context (Mahlis, *et al.* 2005).

The paper is divided into six sections. After the brief introduction, the experimental setup is described then the EMA is presented and the model enabling the linear action block is discussed. The third section concerns the control approach. The control strategy is fuzzy controller, having displacements and velocities as inputs. Section four deals with numerical simulations where a Finite Elements Model (FEM) is used to simulate the dynamic behavior of the studied system in several configurations close to experiment. This step is necessary to build the suitable model for the linear action block and to tune the controller gains. In section five the control block diagram used for numerical simulations is implemented under Dspace[®] environment. The controller implemented is tested experimentally in the context of impact perturbations. Finally, main conclusions are summarized in section six.

2. EMA design and characterization

The experimental setup (Fig. 1) is composed of a flexible steel beam with a constant rectangular section. The beam is clamped at one end and simply supported by a 17000 N/m stiffness cylindrical

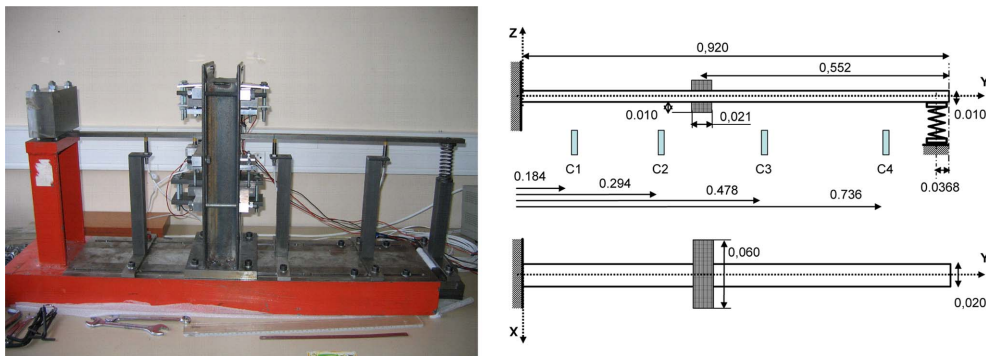


Fig. 1 Experimental setup

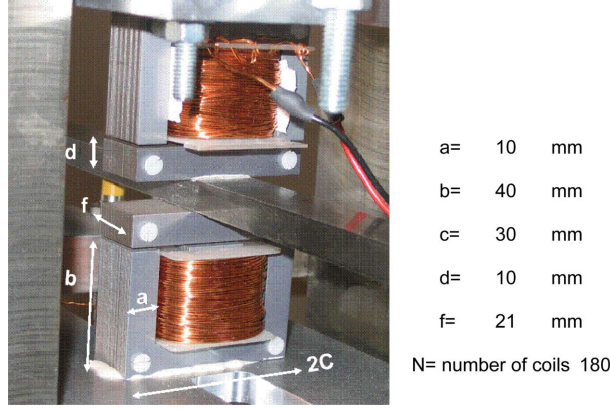


Fig. 2 EMA details

spring at the other end. The actuators are placed 0.368 m from the clamped end. This position is chosen as a function of the mode shape so that the actuators influence the first four modes.

The displacements are measured by using four proximity sensors (Vibrometer TQ 102) located along the y axis, namely, C1 to C4. Their positions are chosen as a function of the mode shape of the first four modes. Real time data acquisition and signal processing is performed by using the A/D-D/A and DSP Dspace® specialized cards. The sampling frequency is 4 kHz and is high enough to avoid using anti-aliasing filters for the frequency range studied.

Since an EMA can only produce attractive forces, two identical actuators commanded independently are necessary. Each EMA is composed of a ferromagnetic circuit and an electrical circuit. The ferromagnetic circuit is composed of two parts; an (E) shape that receives the induction coil and an (I) shape part that is fixed on the beam. Both parts are composed of assemblies of insulated ferromagnetic sheets. The quality of the ferromagnetic circuit alloy is considered high enough and the nominal air gap between the stator and the beam is small enough to consider magnetic loss as negligible. The geometries of the actuators are summarized in Fig. 2.

Actuators are designed to deliver a maximum attraction force of 300 N, and a maximum possible current is 3.0 A. The control input could be either current or voltage, for practical reasons and in order to simplify the electrical EMA model; we chose a current control configuration. The current of each actuator is delivered by two independent amplifiers that convert the input voltage into an output current with 0.3 A/V gain.

As the controller output is the command force, an “inverse model” of each actuator is used. This enables generating the command current that produces the desired command force. Based on magnetic circuit theory and assuming negligible eddy current effects and conservative flux, the relationship between the electromagnetic force (F_{em}), air gap (e), gap distance (δ_a) and current (I) can be expressed as:

$$F_{em} = \frac{N^2 \mu_0 a f I^2}{2 \left((e \pm \delta_a) + \frac{b + c + d - 2a}{\mu_r} \right)} \quad (1)$$

(a , b , c , d and f) correspond to the geometrical characteristics of the actuator and μ_0 is the magnetic permeability of a vacuum ($4\pi \times 10^{-7}$ H/m). μ_r is the relative magnetic permeability (dimensionless) that is a function of the air gap and can be varied according to temperature. Its value is based on manufacturer's specifications and is generally not known with great accuracy. In order to determine its value experimentally,

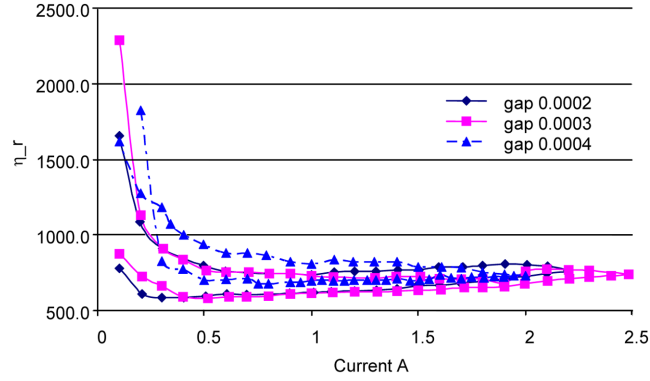


Fig. 3 Relative magnetic permeability versus current for several air gaps

the force generated by an actuator is measured for several air gaps for different increasing and decreasing input current (Fig. 3). In the model presented here, the relative permeability is assumed to be constant for low flux density and the mean value determined for the model is 740. It should be noted that a residual current value subsist even for zero input current. This residual current due to the technology of the amplifiers used is undesirable in our case and must be considered in the model in order to avoid all instability risks.

Once the relative magnetic permeability has been determined, the generated force due to an increasing and decreasing input current is measured for several air gaps (Fig. 4). The hysteresis effects seem to be negligible and the generated forces are obviously proportional to the current square value.

Without an accurate value of the gap distance between the (I) part fixed on the beam and the (E) part it is not possible to determine the applied magnetic force with acceptable accuracy. This distance is rebuilt by using a passage matrix $[H]$ stemming from a cubic interpolation of the modes considered for the structure:

$$[H] = g(y_i, y_a, \phi) \quad (2)$$

Where y_i is the position of the i^{th} sensor, y_a the actuator position and $[\phi]$ is the matrix of the modes considered issued from the finite elements model. In this study the mode shapes are considered for the

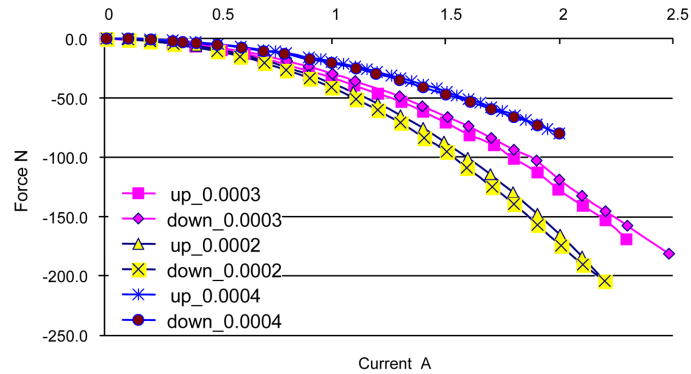


Fig. 4 Measured forces versus current for several air gaps

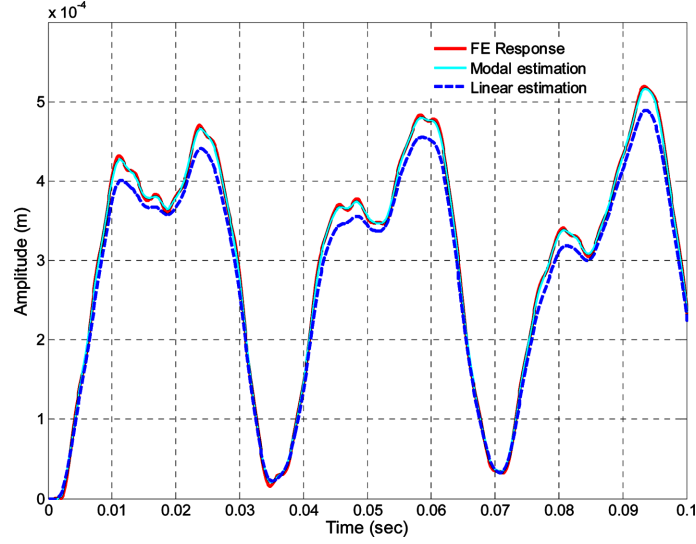


Fig. 5 Modal and linear estimation of actuator air gap

first four modes only, which correspond to the utilization frequency range. The gap distance δ_a is then calculated in function of the measured displacements $\{\delta\}$ as:

$$\delta_a = [\phi]^{-1} \{\delta\} [H] \quad (3)$$

In Fig. 5 the gap distance calculated by using a finite element model is compared with that rebuilt either by modal estimation as described previously, or by linear interpolation of the displacements calculated at nodes #9 and #14, that correspond to the positions of sensors C2 and C3, placed on each side of the EMA. The modal estimation provides an acceptable accuracy and it is the approximation used for the numerical and the experimental investigations.

3. Control approach

The control strategy is a fuzzy controller having displacements and velocities as inputs (Fig. 6).

The principle first consists of the fuzzification of the physical inputs. Each physical input is converted into several fuzzy variables. The number on fuzzy variables depends on the number of membership

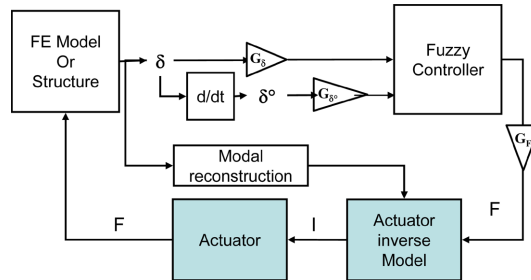


Fig. 6 Diagram of the control strategy

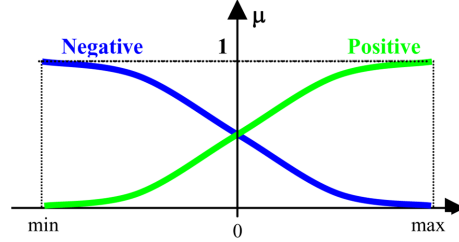


Fig. 7 Input membership functions

Table 1 Fuzzy controller rules

Rule	Condition	Decision
1	IF Positive displacement AND positive velocity	Action
2	IF Positive displacement AND negative velocity	No action
3	IF Negative displacement AND positive velocity	No action
4	IF Negative displacement AND negative velocity	Action

functions used. In this work two membership GBELL Matlab[®] functions “Positive” and “Negative” are used (Fig. 7). The inference engine implements the “minimum” function w_j . Then the rules that characterize the controller are defined (Table 1). Finally the command is obtained after defuzzification. This defuzzification requires the knowledge of the fuzzy output variables corresponding to the rules and the aggregation of these rules as well as the output membership functions. In this paper the Takagi-Sugeno method is used for its well adaptation to the controller real time computation. The member functions are the following:

$$z_1 = 0 \quad \text{and} \quad z_2 = \delta_a + 10\dot{\delta}_a \quad (4)$$

where δ_a and $\dot{\delta}_a$ are respectively the real time radial gap distance displacement and velocity. The command force F is given by the output of the controller used and can be written as:

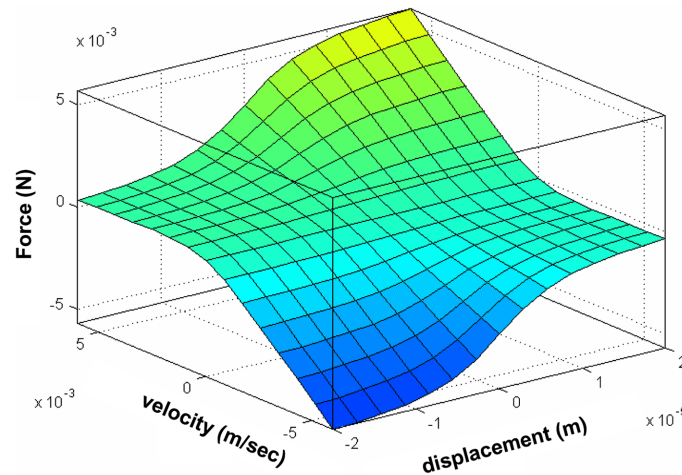


Fig. 8 Fuzzy controller surface

$$F = \frac{\sum_{j=1}^2 w_j z_j}{\sum_{j=1}^2 w_j} \quad (5)$$

The area of the command force related to the displacement and the velocity is shown in Fig. 8.

The controller gains G_{δ} , G_{δ° and G_F are tuned, by using the impact response by using numerical simulations after which they are experimentally adjusted by using the impact response of the structure studied.

4. Numerical investigations

This step is necessary in order to adjust and evaluate the control approaches developed. Numerical simulations are performed in a configuration as similar as possible to the experiments. In order to simulate the measured responses, the structure under study is modeled by using finite elements. The beam is modeled by using 25 equal length Timoshenko beam elements with two nodes and 4 degrees of freedom, namely, two displacements and two rotations per node (Lalanne, *et al.* 1983). The spring is modeled by a supplementary stiffness element placed at node #25. Simulations are carried out under Matlab[®] and Simulink[®] environments. The structure has four bending modes in the frequency range studied, the damping factor is chosen as being equal to 0.003 for all modes (Table 2).

The fuzzy controller gains are adjusted by using the FEM. Several control configurations were assessed; final results are only presented in this paper.

Table 2 Characteristics of the model

Mode	Frequency (Hz)	Damping factor
1	28.15	0.003
2	58.57	0.003
3	155.81	0.003
4	317.02	0.003

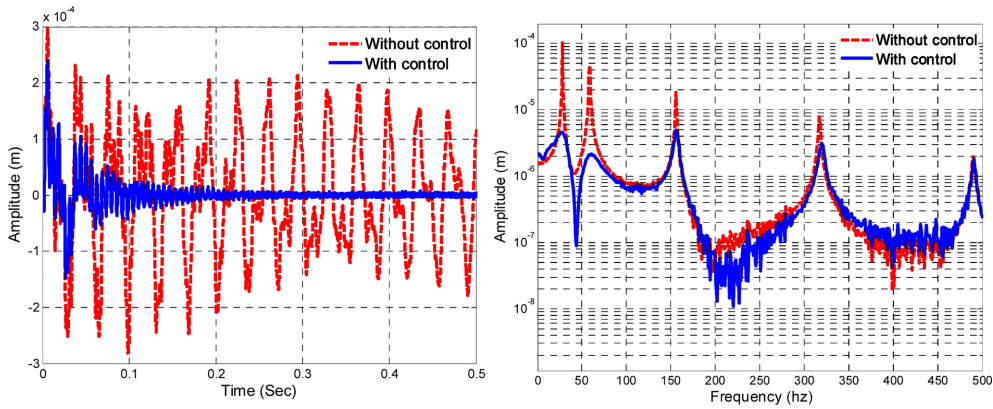


Fig. 9 Impulse responses, with and without control, node #14

To be as similar as possible to experiments, band-limited white noise is superposed on the calculated displacements. The root mean square value of the added noise is 3.2×10^{-6} m. The velocities are obtained by numerical derivation of the displacements.

The impulse responses of the system, with and without control, for node #14 that correspond to the sensor C3 are presented in Fig. 9. The controller and the linear command block seem to be efficient; the amplitude attenuation is obtained for a period less than 0.2 second. Same trends are observed for the nodes corresponding to the other sensors.

By observing the responses in frequency domain, we can conclude that the amplitude levels are attenuated especially for the first four modes. On the other hand, results show that there are no control spillover effects.

5. Experimental investigations

The block diagram established and used for the numerical simulations is implemented under Dspace[®] environment. It comprises a calculation and information management card DS1005, equipped with a processor DSP TMS320C40, a data acquisition card DS2002 (12 bits and conversion time of $3.3 \mu\text{s}$) and a restitution of data card DS2101 (12 bits and conversion time of $3 \mu\text{s}$). All these cards are plugged in a Dspace car-box connected to a PC and are emulated in the Matlab[®] - Simulink[®] environment. The sampling rate used is 3 kHz.

The impulse responses are obtained by using an impact hammer Brüel & Kjaer (B&K 8202) with a piezoelectric force sensor (B&K 8200). The sampling frequency is 4096 Hz. The measurements are repetitive and the maximum variation coefficient (standard deviation/mean) of the frequencies is less than 2%.

The residual current is considered in the model of the linear command block. The values measured are different for each actuator; this difference is considered in the actuator inverse model in order to avoid any risks of instability.

The gap distance between the (I) part fixed on the beam and the (E) part is rebuilt by using the

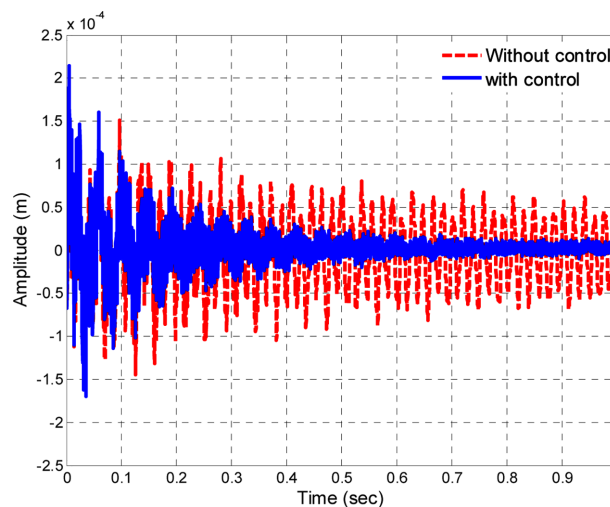


Fig. 10 Time domain, impulse responses, with and without control, sensor C3

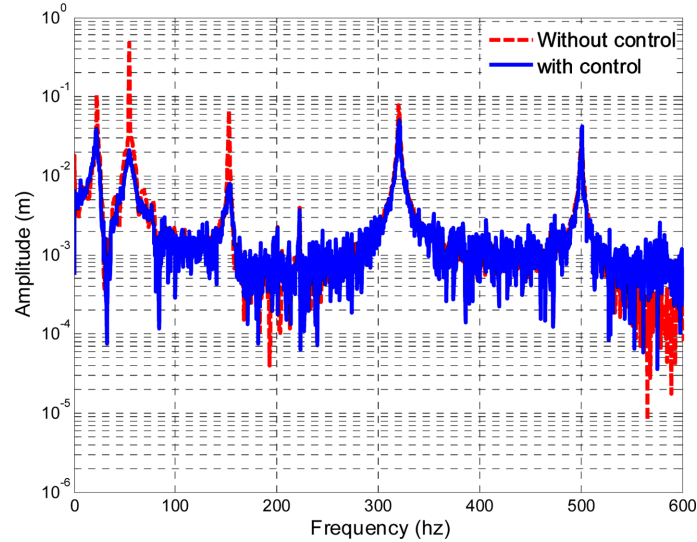


Fig. 11 Transfer function, impulse responses, with and without control, sensor C3

passage matrix $[H]$ stemming from the cubic interpolation of the considered modes as described in the numerical investigations. The matrix of mode shapes is obtained from the FEM.

The control approach is evaluated for an impulse impact excitation generated by applying the impact hammer 0.22 m from the clamped end. Applying the impact at this position enables the excitation of a large frequency band. The impulse responses measured by sensor C3 are compared with and without control (Fig. 10). The controller and the actuator inverse model seem to be efficient; the amplitude attenuation is obtained for a period less than 0.4 second. Same trends are observed for the other sensors.

The transfer function of the measured response is examined in Fig. 11. The controller enables an important reduction of the amplitude levels for the three first modes, the fourth mode level is slightly attenuated and there is no effect on the higher modes, consequently the control spillover effects are limited.

6. Conclusion

In this paper an ElectroMagnetic Actuator (EMA) is designed and characterized experimentally. The EMA is designed as a function of the experimental structure to be controlled. In order to have a linear action block, an inverse model of the actuator, based on magnetic circuit theory, is used. It enables to generate the command current that produces the desired command force. The gap distance is estimated by cubic modal interpolation of the measurements stemming from all sensors.

A residual current value subsists even for zero input current. This residual current is due to the technology of the amplifiers utilized and is undesirable in our case. The residual current is measured and considered in the model in order to avoid any risk of instability.

The observation of the generated force by the EMA, due to an increasing and decreasing input current, shows that the hysteresis effects are negligible. Moreover, the generated forces are obviously proportional to the current square value.

Then the possibility of controlling a flexible beam is assessed numerically and experimentally. The

numerical simulations enable a better comprehension of the basic phenomena and permit evaluating several approaches and thus the selection of the most efficient for the experimental evaluation. The control strategy is a fuzzy controller having displacements and velocities as inputs. The controller and the actuator inverse model seem to be efficient; important amplitude attenuation is obtained. The control spillover effects are limited.

Researches are going on in order to apply the EMA technology in conjunction with conventional support bearings for the control of dynamic behavior of rotating machinery.

Acknowledgement

The authors would like to thank Miss C. Beau, laboratory technical assistant, for her invaluable help.

References

- Aenis, M., Knopf, E. and Nordmann, R. (2002), "Active magnetic bearings for the identification and fault diagnosis in turbomachinery", *Mechatronics*, **12**, 1011-1021.
- Couzon, P.Y. and Der Hagopian, J. (2007), "Neuro-Fuzzy active control of rotor suspended on active magnetic bearing", *J. Vib. Control*, **13**(4), 365-384.
- El-Shafei, A. and Dimitri, A.S. (2007), "Controlling journal bearing instability using active magnetic bearings", *Proc. of ASME Turbo Expo*, GT2007-28059, Canada.
- Forrai, A., Ueda, T. and Yumura, T. (2007), "Electromagnetic actuator control: a linear parameter-varying (LPV) approach", *IEEE T. Cont. Syst. T.*, **54**(3), 1430-1441.
- Fung, R.F., Liu, Y.T. and Wang, C.C. (2005), "Dynamic model of an electromagnetic actuator for vibration control of a cantilever beam with a tip mass", *J. Sound Vib.*, **288**, 957-980.
- Kasarda, M., Mendoza, H., Kirk, R.G. and Wicks, A. (2004), "Reduction of subsynchronous vibrations in a single-disk rotor using an active magnetic damper", *Mech. Res. Commun.*, **31**, 689-695.
- Kasarda, M., Marshall, J. and Prins, R. (2007), "Active magnetic bearing based force measurement using the multi-point technique", *Mech. Res. Commun.*, **34**, 44-53.
- Lalanne, M., Berthier, P. and Der Hagopian, J. (1983), *Mechanical vibrations for engineers*, A Wiley-Interscience publication, 266 p.
- Lee, S.Q. and Gweon, D.G. (2000), "A new 3 DOF Z-tilts micropositioning system using electromagnetic actuators and air bearings", *Precis. Eng.*, **24**, 24-31.
- Lei, S. and Palazzolo, A. (2008), "Control of flexible rotor systems with active magnetic bearings", *J. Sound Vib.*, **314**(1-2), 19-38.
- Liu, J. and Liu, K. (2008), "Application of an active electromagnetic vibration absorber in vibration suppression", *Struct. Control Health Monit.*, DOI: 10.1002/stc.288.
- Mahlis, M., Gaudiller, L. and Der Hagopian, J. (2005), "Fuzzy modal active control of the dynamic behavior of flexible structures", *J. Vib. Control*, **11**, 67-88.
- Mani, G., Quinn, D.D. and Kasaeda, M. (2006), "Active health monitoring in a rotating cracked shaft using active magnetic bearings as force actuators", *J. Sound Vib.*, **294**, 454-465.
- Matsuzaki, Y., Ikeda, T., Nae, A. and Sasaki, T. (2000), "Electromagnetic forces for a new vibration control system: experimental verification", *Smart Mater. Struct.*, **9**, 127-131.
- Schweitzer, G., Bleuler, H. and Traxler, A. (2003), *Active magnetic bearings - basics, properties and applications*, pdf Hochschulverlag AG, ETH, Zurich.
- Simões, R.C., Der Hagopian, J., Mahfoud, J. and Steffen Jr, V. (2007), "Modal active vibration control of a rotor using piezoelectric stack actuators", *J. Vib. Control*, **13**(1), 45-64.